Paleoceanographic Variability of the North Atlantic from Marine Isotope Stage 6 to 5 at Integrated Ocean Drilling Program suptropical Site 1313 and subpolar Site 1314

Senior Thesis
Submitted in partial fulfillment of the requirements for the
Bachelor of Science Degree
at The Ohio State University

By

Mary Elizabeth Smith
The Ohio State University
2010

Approved By

Harunur Rashid, Advisor
Lawrence L. Krissek
Byrd Polar Research Center
School of Earth Sciences

TABLE OF CONTENTS

Abstract:

The North Atlantic Ocean plays a crucial role in shaping the terrestrial climates of the Northern Hemisphere. The penultimate deglaciation (140 to 130 ka B.P.) is considered as one of the most rapid oceanographic changes of the Quaternary period. Past changes in ocean circulation are mainly obtained by analyzing deep sea sediments using various proxies. In this study, we reconstruct the variability in the upper water masses of the North Atlantic by analyzing Integrated Ocean Drilling Program (IODP) sediment cores retrieved from a subpolar (1314) and subtropical (1313) location from Marine Isotope Stage (MIS) 6 to 5 (180-120 ka B.P.). Planktonic foraminifera are well-linked to climatic and environmental conditions in this area and serve as a paleo-proxy for oceanographic variability. Variability in sea-surface conditions and associated water masses are reflected by changes in fossil planktonic foraminiferal relative abundances. The $\delta^{18}O$ of planktonic foraminifera is used to indicate relative warmer and cooler sea-surface conditions. Iceberg input is inferred by the presence of ice-rafted debris. The variability of the North Atlantic Current and the Polar Front was assessed by tracking the migration of subtropical and subpolar waters. We find clear indications of freshwater inputs, including a Heinrich Event, which provide a mechanism to freshen the sea-surface and perturb conditions. The warmest sea-surface conditions appear in phase with interglacial MIS 5 and the coolest conditions appear in phase with glacial MIS 6. Our results indicate that the North Atlantic surface circulation responds to changing conditions associated with a transition from a glacial to interglacial period.

Acknowledgements

I would like to acknowledge and thank the Integrated Ocean Drilling Program for providing samples for this study, the Biogeochemistry Laboratory of OSU for stable isotope analysis and funding from the OSU Arts & Sciences Undergraduate Research Scholarship. Thank you to Wesley Haines for his technical computer support, Rachael Gray and Kevin Crawford for their ideas and support, and Larry Krissek for advising guidance. Special thanks to Leonid Polyak for letting me use his equipment and lab at the Byrd Polar Research Center. And lastly, very special thanks to my advisor Harunur Rashid for his guidance and support but above all for his intellect and patience in taking on an average student.

List of Figures

List of Tables

1) Introduction

Glacial Cycles

Large ice sheets have dominated the Northern Hemisphere for the last million years of Earth's history. The Pleistocene epoch (1.8 Ma -11.5 ka) is characterized by many Northern Hemisphere ice sheets advance and retreat, giving way to the glacial cycles discovered from the geologic record. The glacial cycles are attributed to periodicities in Earth's orbit that influence the amount of incoming solar radiation (Milankovitch, 1941) thus contributing to changes in other processes such as ice-albedo feedbacks and ocean circulation.

During the last 0.9 million years, Earth has gone through eight ice age cycles occurring at 100,000 year intervals (Serreze & Barry, 2005). During glacial intervals, climates are characterized by extreme millennial-scale variability; rapidly changing from cold to relatively warmer conditions. These high frequency changes are known as D/O cycles (Dansgaard et al., 1993). The transition from glacial to interglacial conditions, known as a termination, can occur in as little as 10,000 years (Ruddiman, 2008). The last interglacial period, known as the Eemian, is thought to be characterized by a climate with temperatures as warm as today (Kukla et al., 2002). The last interglacial has been correlated to Marine Isotope Stage (MIS) 5e (Shackleton et al., 2003). Marine Isotope Stages refer to paleoclimate histories of warm and cold periods denoted by an odd or even number respectively. In this study, we have focused on the deglaciation from MIS 6 to 5 (the penultimate deglaciation) corresponding to 180,000-120,000 yr B.P.

Marine Geologic Record

Marine sediment cores across the North Atlantic Ocean provide a paleo-environmental record of the glacial cycles and ensuing changes in ocean circulation for this region. Research from analyzing cores has shown that the oceans play a dominate role in modulating global climate change**.** The North Atlantic plays a crucial role in shaping the climates of the Northern Hemisphere. The surface current known as the Gulf Stream transports heat and moisture from the tropics to higher latitudes. It is the northern extension of this current that is primarily responsible for the warmer climate of northwestern Europe today. Past changes in ocean circulation are mainly derived by analyzing deep sea sediments. Marine sediment is comprised of marine biological remains and continental derived material. Sediment collected from the ocean floor records environmental variability through time which can be reconstructed with various proxies.

Paleoceanographic Proxies

Within the sediment that accumulates on the sea floor are the shells of microscopic marine organisms called planktonic (surface dwelling) foraminifera. When these organisms die their calcite shells become preserved as fossils within the sediment. Foraminifers live within different ranges of temperature and depth in the water column. The schematic diagram in Figure 1 illustrates the various depth habitats and associated currents of the foraminifera used in this study.

Foraminifera characterize distinct biogeographic zones which are linked to particular water masses (Kreveld, 1996). The presence of a specific species in the fossil record will indicate a past warmer or cooler water environment by comparison with data from modern analogs. For example, the deep-dwelling species *Neogloboquadrina pachyderma* sinistral (s) indicates cold conditions as it is a proxy for polar water masses (Kreveld, 1996). The presence of surface dwelling *Globigerina bulloides* indicates subpolar to temperate conditions and is associated with the North Atlantic Current (NAC) (Kreveld, 1996). *Neogloboquadrina pachyderma* dextral (d) indicates subpolar conditions and is also associated with the NAC (Kreveld, 1996). The subtropical species *Globorotalia inflata* is especially important for this study as it lives in the base of the thermocline and is associated with the NAC and Gulf Stream (Cléroux et al., 2007). In addition to planktonic foraminfera, benthic (bottom dwelling) fauna also provide a useful proxy for time constraint. The oxygen isotope ratio of benthic foraminifera is generally interpreted as a record of terrestrial ice volume.

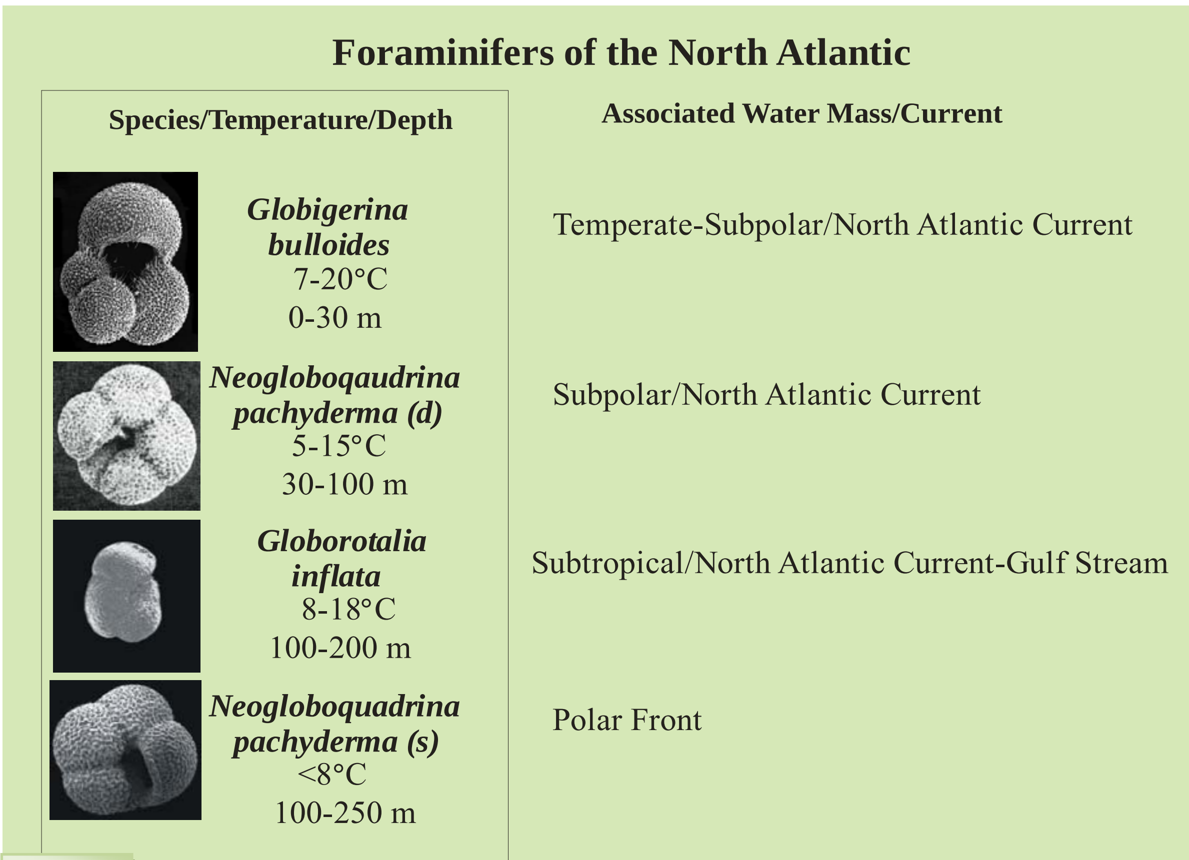

Figure 1 Schematic representation of various species of planktonic foraminifers from the North Atlantic as a function of water depth (d'Orbigny; Ehrenberg; Rashid and Boyle, 2008; Ottens, 1991; Bé and Tolderlund, 1997; Cleroux et al 2007; Kreveld, 1996).

The isotopes ^{18}O and ^{16}O are incorporated from the ocean water into the calcite ($CaCO_3$) tests of foraminifera. The ratio of $^{18}O/^{16}O$ is a function of the temperature and ocean water composition during test calcification (Emiliani, 1966). Isotopic fractionation is responsible for the preferential uptake of either ^{18}O or ^{16}O. Water is transferred via the hydrologic cycle from ocean to land, where it can be stored as ice. The heavier ^{18}O evaporates less readily; thus ^{16}O is preferentially removed, leaving the water enriched in ^{18}O. The $\delta^{18}O$ of foraminifera are compared to a standard and given in per mil (‰) deviation from the standard by the following equation:

$$\delta^{18}O = \frac{(^{18}O/^{16}O)_{Sample} - (^{18}O/^{16}O)_{Standard}}{(^{18}O/^{16}O)_{Standard}} \times 10^{3}$$

Enriched $\delta^{18}O$ values of benthic foraminifera represent larger ice volume on the continent whereas depleted $\delta^{18}O$ values represent less ice. The global benthic oxygen isotope stack of Figure 2 shows multiple transitions from more ice volume to less, corresponding to glacial and interglacial cycles. The grey highlighted area represents the penultimate deglacial sequence (MIS 6 to 5) of this study.

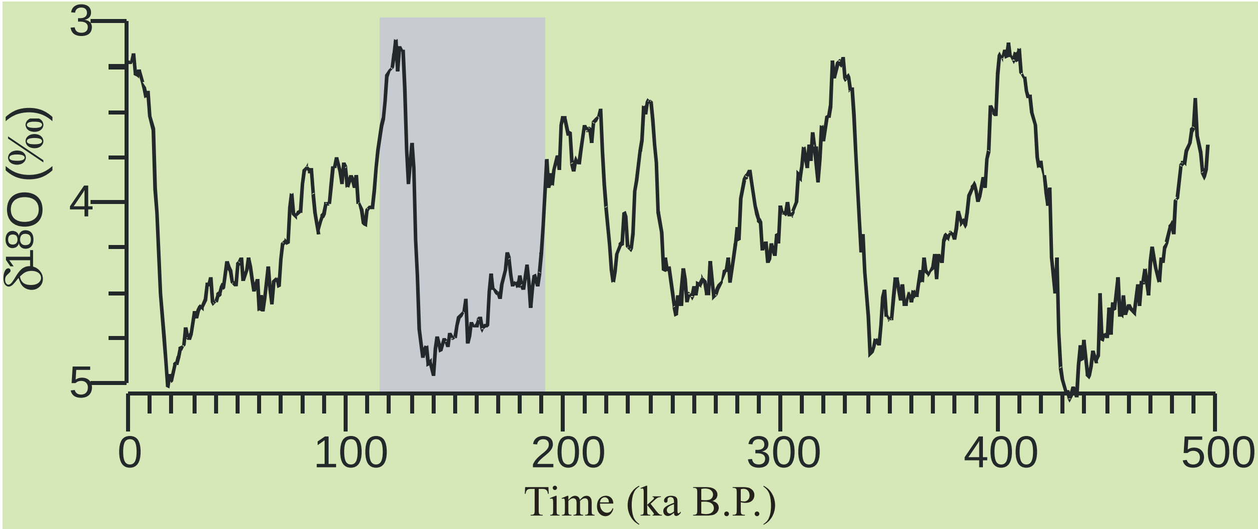

Figure 2 Global Benthic Stack: Stable Oxygen Isotope values determined on benthic foraminifera represent ice-volume changes during the last 500 ka B.P. Enriched values represent more ice/cold glacial peri ods, whereas depleted values represent less ice/warmer interglacial periods. Penultimate deglacial sequence (MIS 6&5) highlighted in grey.(Lisiecki & Raymo, 2005)

Sediment cores also contain records of major ice-sheet collapse and iceberg rafting. Ice-rafted debris (IRD) appears within the sediment as tiny rock fragments. These fragments are interpreted as the debris deposited from melted icebergs (Fig. 3). Icebergs are an important component in sea-surface freshening as the melt-water reduces the sea-surface salinity of the ocean. Most fragments of North Atlantic IRD appear to originate mainly from Iceland, west Greenland and other small coastal ice-shelves (Bond & Lotti, 1995). This indicates that icebergs have a tendency to calve in high frequency from the ice-sheets in these areas.

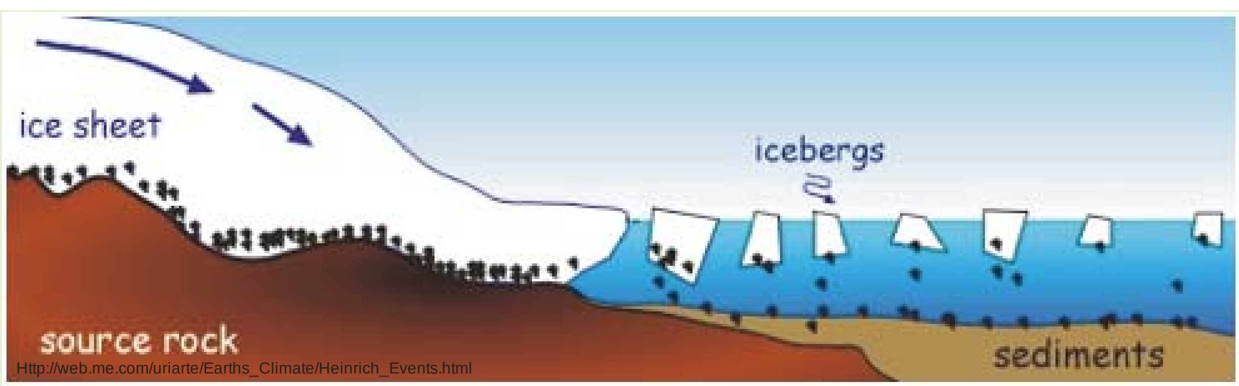

Figure 3 Schematic representation of the ice-shelf, iceberg discharge and deposition of IRD in marine sediment (web.me.com/uriarte/Earths_Climate/Heinrich_Events.html).

A massive discharge of icebergs, called a Heinrich Event, is inferred by the presence of detrital carbonate IRD. This type of large freshwater event originated from icebergs of the Laurentide ice-sheet via the Hudson Strait (Heinrich, 1988; Broecker, 1994). Several Heinrich Events have been identified in the glacial cycles of the Pleistocene, including Heinrich Event 11 (H11) which occurred during the penultimate deglaciation.

2) Oceanographic Setting

The North Atlantic and Thermohaline Circulation

The North Atlantic is considered as one of the most climatically sensitive regions due to its key role in thermohaline circulation. The North Atlantic Current is the northern extension of the Gulf Stream and is an important northeast flowing current. It helps separate the cold waters of the Polar Front from the warmer subtropical waters (Thornalley et al., 2009). As the NAC approaches high latitudes it cools and releases moisture. It becomes more saline and dense, thus sinking in the Norweigian-Greenland Seas (NGS) forming North Atlantic Deep Water (NADW). This contrast in density causes the NAC to sink and pull warmer water farther north. The resulting NADW returns south as a deep water current driving the conveyor belt-like process called thermohaline circulation (THC). This modern circulation pattern can be seen in Figure 4. THC follows strong NAC activity as an efficient positive feedback (Labeyrie et al., 1999). However, in the past this configuration has been perturbed.

Enhanced melt-water discharge into the North Atlantic contributes to the freshening of the NGS. This surface freshening reduces deep convection and NADW production (associated with strong thermohaline circulation) producing a widespread cooling (Broecker et al., 1990). This scenario allows the Polar Front to migrate south (Johannessen et al., 1993). The NAC and

Polar Front have been found to oscillate in parallel with the North American ice-sheets (Labeyrie et al., 1999) and thus glacial cycles. During glacial periods, the Polar Front migrated south from the Arctic resulting in a southern shift of the NAC/Gulf Stream (Johannessen et al., 1993). As a result, this may have reduced the transportation of heat to higher latitudes.

The ocean is divided vertically into distinct water masses based on temperature gradients. Water warmed by the sun is less dense and remains on the surface. This layer is referred to as the

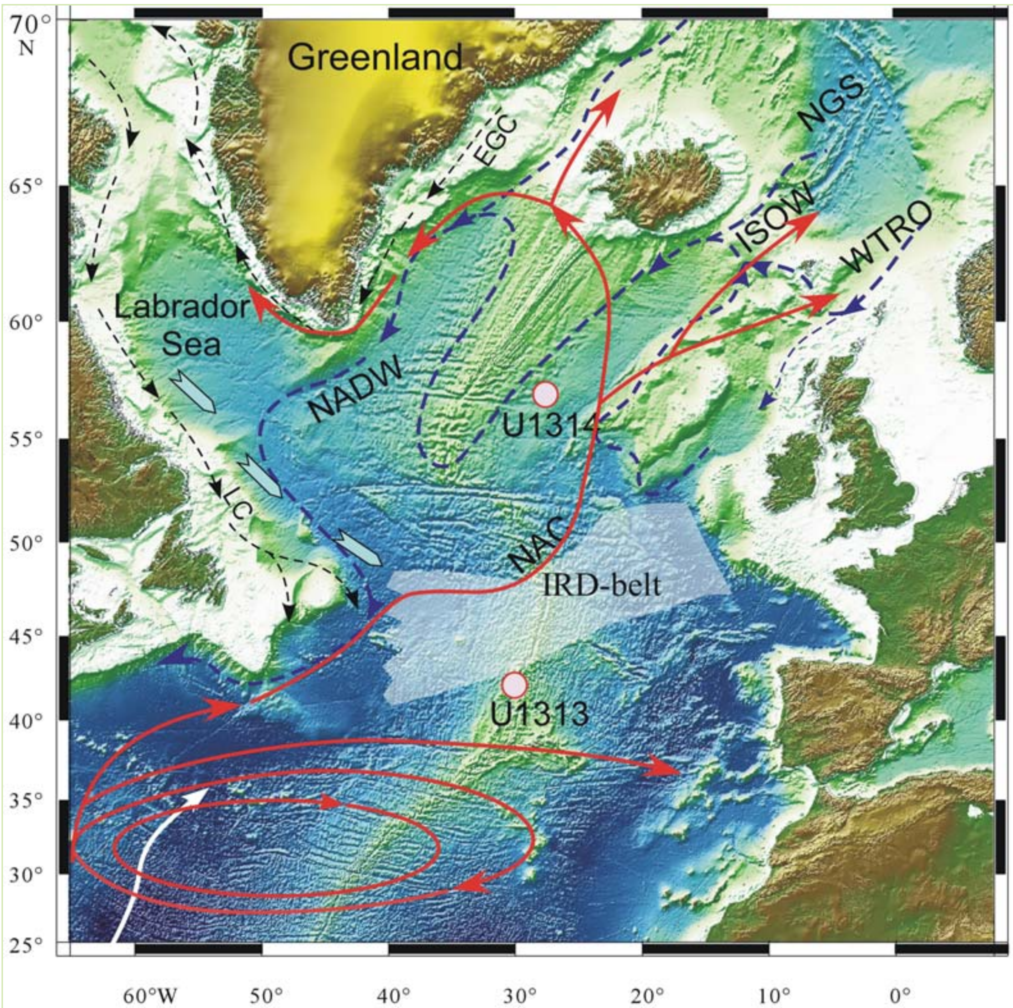

Figure 4: Location of cores discussed in this study are shown. Iceberg trajectory (thick blue arrows), Labrador Current (LC), and East Greenland Currents (EGC), and the North Atlantic Current (NAC) (thick red solid lines) paths are shown. Position of the subtropical gyre in the western Atlantic is shown by red lines. Location of ice-rafted detritus (IRD) belt shown by gray-shaded area, iceberg routes and NAC are drawn according to Ruddiman (1977). Blue discontinuous lines are the presumed routes of the North Atlantic Deep Water (NADW) flow. NGS: Norwegian-Greenland Seas; WTRO: Wyville-Thompson Ridge Overflow; ISOW: Icelandic Overflow Water.

mixed layer. Separating the upper mixed layer from the deep water is an intermediate layer where temperatures decrease rapidly with depth. It is known as the thermocline. The thickness of this layer varies based on changes in surface water conditions and/or seasonality. The mixed and thermocline layers are responsible for the ocean's heat storage and transportation (Cléroux et al., 2008). Consequently, it is important to understand the variations in the upper water column as this is where most energy storage and heat transport occur.

3) Objective

In this study we have chosen to track the continuously changing environmental conditions throughout MIS 6 to 5 using subtropical and subpolar IODP sites 1313 and 1314 in the North Atlantic. IODP core sites 1313 and 1314 were drilled at the western flank of the mid-oceanic ridge (41.006°N, 32.574°W; 3,426 mwd) and the Gardar Drift (56.36°N, 27.88°W; 2,820 mwd), respectively (Fig. 4). The deglacial sequence investigated in this study has been correlated to specific depth intervals within the sediment cores. To ensure a diverse selection of foraminifer species across the deglaciation, core sites were drilled outside the 'IRD-belt' (Ruddiman, 1977). Site 1313's subtropical location will reveal when the Polar Front migrated south, whereas site 1314 will reveal when warm water inflow (associated with the NAC) was dominant. The sites will reveal the latitudinal extent of past sea-surface variability demonstrating the complex interplay of colder versus warmer water masses.

Our focus is to reconstruct the structure of the upper water masses throughout this interval. The relative abundances of planktonic foraminifera will be used to detect the migration of tropical waters during warmer periods and subpolar waters during colder periods. The variability of iceberg input will be monitored by IRD. The $\delta^{18}O$ in planktonic foraminifera represents the temperature and salinity of the seawater during the formation of their tests.

Enriched $\delta^{18}O$ values indicate cooler temperatures, whereas depleted $\delta^{18}O$ values indicate warmer temperatures or surface water freshening by meltwater. The $\delta^{18}O$ of planktonic species *G. bulloides* and *G. inflata* will be used to assess various conditions as well as water column stratification.

From this study, we will assess the dynamics of the oceanic fronts during a colder (MIS 6) or warmer (MIS 5) climate. Changes in the upper water masses have been correlated to abrupt climate changes in the North Atlantic. By studying this time interval we will gain insight into the future dynamics of climate. If glacial cycles and millennial oscillations prove to be cyclic, it will be useful in predicting the natural course of climate change into the future.

Furthermore, over the past decade, scientists have acquired evidence to suggest that the Earth's average air and sea temperatures are rising as well as the sea level. This has been attributed to increased atmospheric CO_2 concentration and melting of the Greenland and Antarctic ice sheets. Climatic changes have a major consequence for humanity as our species was only able to thrive after coming out of the last ice age around 11,000 yr BP. The abrupt nature of some of these shifts can occur within human life spans as is evident from modern research. While the modern climatic shift can be ascribed to anthropogenic forcing, it is necessary to understand this modern change in context of the past. By documenting the natural variability of climates in the past we can gain a better understanding about the future mechanisms of change. Therefore, this study was conducted on a time interval that might serve as an analogue to the modern climate.

4) Methods

Sampling Methods

Sediment samples for this study were collected from the North Atlantic during the IODP expedition 306 from sites 1313 and 1314. Cores were sampled at 2 cm sediment intervals. Site 1313 was studied between the 565-915 cm depth interval and site 1314 was studied between the 1000-1328 cm depth interval. Samples were dried in an oven at 64°C for 48 hours and then weighed. Samples were wet sieved using a > 63 μm sieve and ultrasonicated to remove clay and other fine particles. The washed residue was then sieved again at > 150 μm size fraction for foraminiferal and IRD counts.

To obtain abundance counts of 300-600 foraminifera, the washed residue was split using a microsplitter. The number of splits was recorded for use in determining the relative abundance of each species based on estimated total foraminifera per sample. Using a binocular microscope, various species of planktonic foraminifera were identified and counted including: *Neogloboquadrina pachyderma* sinistral (s), *Neogloboquadrina pachyderma* dextral (d), *Globigerina bulloides* and *Globorotalia inflata.* (Kenett and Srinivasan, 1983). In addition to foraminifera, shell fragments and IRD were counted. IRD petrology was assessed to identify a Heinrich Event based on the presence of detrital carbonate (Bond et al., 1993; Rashid and Boyle, 2007).

Laboratory Procedures

Stable oxygen isotope ratios were determined on *G. inflata* in a 150-250 µm size fraction for sites 1313 and 1314. The frequency of sampling varies (*G. inflata* is absent in MIS 6 at 1314) but 104 and 20 samples were analyzed throughout the 1313 and 1314 intervals respectively with 36 standards and replicates. Approximately 30 specimens of *G. inflata* were picked to ensure proper weight for mass spectrometer analysis and for future use in replicating isotopic results. Because foraminifera exhibit variability in test morphology and weight, different numbers of specimens are used per sample to obtain the required weight for the isotopic analysis. The combined weight of the foraminifera must fall within 80 and 100 micrograms per sample for stable isotope ratio mass spectrometer analysis.

Oxygen and carbon stable isotopes were analyzed in the Stable Isotope Biogeochemistry Laboratory of Dr. Grottoli in the School of Earth Sciences. Each sample was analyzed for $\delta^{18}O$ ($\delta^{18}O$ = per mil deviation of ^{18}O:^{16}O) relative to NBS 18, 19 and 20 standards using an automated carbonate Kiel extraction device coupled to a Finnigan Delta IV Plus stable isotope ratio mass spectrometer. Samples were acidified under vacuum with 100% ortho-phosphoric acid, the resulting CO_2 cryogenically purified, and delivered to the mass spectrometer. Approximately 10% of all samples were run in duplicate. The standard deviation of repeated measurements of an internal standard was ±0.06 ‰for $\delta^{18}O$.

Paleoceanography of site 1313

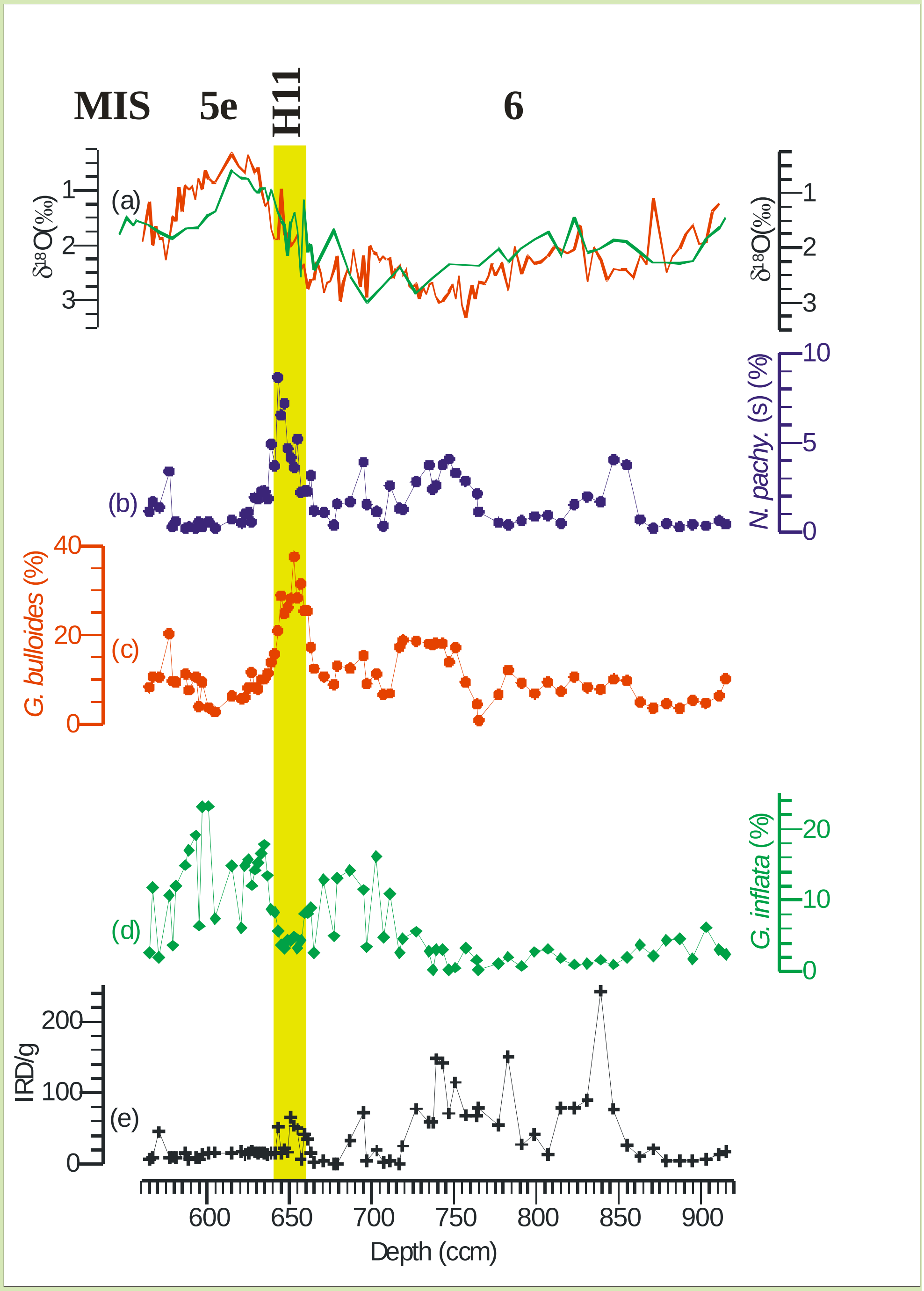

Figure 5: Plots of (a) $\delta^{18}O$ *G. bulloides* (red) *and G. inflata* (green), (b) *N. pachyderma* (s) (%), (c) *G. bulloides* (%), (d) *G. inflata* (%), and (e) IRD are shown as a function of composite depth (ccm) from site 1313. H11 is highlighted by the vertical yellow bar. H11 coincides with a peak in *G. bulloides* and a low abundance of *G. inflata*. The peak of *N. pachyderma* (s) (%) is offset from H11.

5) Results

Site 1313

The $\delta^{18}O$ in *G. bulloides* and *G. inflata* (Fig. 5a) show a typical deglacial sequence from MIS 6 to 5; with enriched values in glacial MIS 6 and depleted values in MIS 5 (and warmer substages of MIS 6). The gradual change in values between isotope stages is identified at Termination II.

IRD is normalized to per gram concentration in Fig. 5e. Four prominent peaks occur in MIS 6. Heinrich Event 11 (H11) is identified halfway through Termination II. However, the mean IRD concentrations of MIS 6 are higher than H11. IRD decreases to background concentrations in MIS 5 (Ruddiman, 1977).

N. pachyderma (s) (Fig. 5b) remains low in abundance (< 5%) throughout MIS 6. It reached a peak maximum of 10% abundance at the end of H11, thus doubling its highest glacial abundance. It rapidly decreased at the onset of MIS 5 becoming nearly absent in the interglacial.

G. bulloides (Fig. 5c) maintains a variable presence throughout both stages with slightly higher abundances in MIS 6. It reached a peak maximum of nearly 40% abundance during H11. It rapidly declined at the onset of MIS 5. The abundance curves of *G. bulloides* and *N. pachyderma* (s) generally follow each other.

G. inflata (Fig. 5d) increased in late MIS 6 to nearly 20% from less than 5%. At H11 it decreased rapidly and reached a minimum of about 5%. At the end of H11, it increased rapidly reaching over 20% abundance in MIS 5. From late MIS 6 onward, *G. inflata* is generally inversely correlated to *G. bulloides.*

In MIS 6, *G. bulloides* generally exhibits more enriched $\delta^{18}O$ values compared to *G. inflata*. During Termination II both species show similar $\delta^{18}O$ values. In MIS 5, *G. bulloides* shows more depleted $\delta^{18}O$ values compared to *G. inflata*.

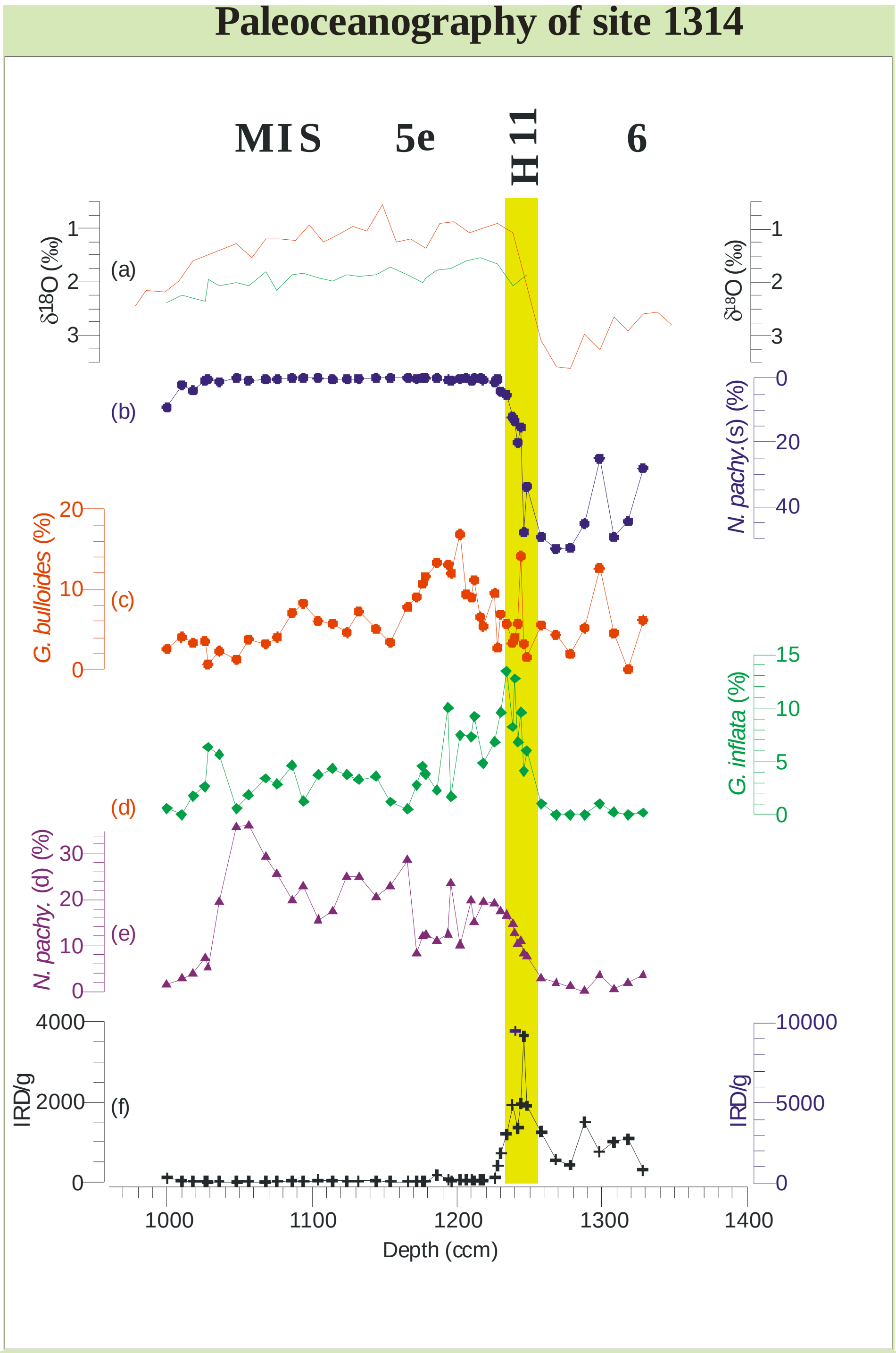

Figure 6: Downcore plots of (a) δ^{18}O in *G. bulloides* (red) and *G. inflata* (green), (b) *N. pachyderma* (s) (%), (c) *G. bulloides* (%), (d) *G. inflata* (%), (e) *N. pachyderma* (d) (%), and (f) IRD are shown from site 1314 as a function of composite depth (ccm). H11 is highlighted by the vertical yellow bar. *N. pachyderma* (s) (%) is inversely correlated to the δ^{18}O curve and *N. pachyderma* (d) follows it.

Site 1314

The $\delta^{18}O$ curve of *G. bulloides* (Fig. 6a) shows a typical deglacial sequence from MIS 6 to 5; with enriched values in glacial MIS 6 (and colder substages of MIS 5) and depleted values in MIS 5. The abrupt change in values between Isotope Stages is identified as Termination II. The depleted values of $\delta^{18}O$ of *G. inflata* reflect the warmer interglacial MIS 5. No *G. inflata* specimens were found within the MIS 6 interval, thus we were unable to reconstruct an isotopic curve for *G. inflata* in this interval.

IRD/g (Fig. 6f) exhibits very high concentrations throughout MIS 6 and reached a maximum halfway through Termination II. This is indentified here as Heinrich Event 11 (H11). IRD exists only in trace amounts in MIS 5.

N. pachyderma (s) (Fig. 6b) displays a general glacial-interglacial trend by inversely following the $\delta^{18}O$ curve of *G. bulloides.* Its highest abundance of over 40% occurred in MIS 6. It rapidly diminished during the Termination remaining absent throughout MIS 5.

G. bulloides (Fig. 6c) exhibits a more variable trend but is present throughout both stages. It maintained a robust peak during the early phase of MIS 5 reaching over 15%.

G. inflata (Fig. 6d) remains nearly absent throughout MIS 6. It reached a maximum of 15% at the end of H11 and remains in higher abundance in early MIS 5. It averages around 5% in the latter phase of MIS 5.

N. pachyderma (d) (Fig. 6e) also displays a general glacial-interglacial trend. The abundances increased rapidly during the Termination with highest concentrations of 30% occurring in late MIS 5. *N. pachyderma* (d) is nearly absent in MIS 6 when *N. pachyderma* (s) is at its highest abundance. Thus, these two species are generally inversely correlated with each other.

In MIS 5, *G. bulloides* shows more depleted $\delta^{18}O$ values compared to *G. inflata*.

6) Discussion

Site 1313

The $\delta^{18}O$ curves of *G. bulloides* and *G. inflata* (Fig. 5a) display enriched values throughout cold glacial MIS 6 and depleted values in warm MIS 5 (and warmer phases of MIS 6). This substantiates the use of planktonic foraminifer $\delta^{18}O$ as a proxy for relative sea-surface conditions/temperature at this site.

H11 produced a distinct change in the abundances of *N. pachyderma* (s), *G. bulloides* and *G. inflata*. This event can be associated with a freshening and/or temporary cooling of the sea-surface. Sea-surface cooling is indicated by the return of polar species *N. pachyderma* (s) and the thriving of subpolar species *G. bulloides*. This is further demonstrated by the sharp decline of temperate species *G. inflata.* The isotopic values for the H11 interval are not at a high enough resolution to show a pronounced effect.

The warmer sea-surface conditions of MIS 5 are marked by the increase of *G. inflata* and subsequent decline in *G. bulloides* and *N. pachyderma* (d).

According to the 'water column stratification index' (Mulitza et al., 1997), the similar $\delta^{18}O$ values of *G.bulloides and G. inflata* in Termination II suggest a mixed water column, without a thermocline. The negative $\Delta\delta^{18}O$ values ($\Delta\delta^{18}O = \delta^{18}O$ *G. bulloides* – $\delta^{18}O$ *G. inflata*) in MIS 5 suggest water column stratification. Stratification indicates the presence of a seasonal (spring-summer) thermocline. A seasonal thermocline will allow heat transport to be restored to higher latitudes by warm surface currents. A stratified water column will allow a strengthening of the surface NAC which is typical of interglacial oceanographic configuration. The abundance increase of *G. inflata* complements this interpretation.

Site 1314

The $\delta^{18}O$ curve of *G. bulloides* displays enriched values throughout cold glacial MIS 6 and cooler phases of MIS 5 near the end of the interglacial. Both $\delta^{18}O$ curves display depleted values during the warm MIS 5 (Fig. 6a). The steep nature of the Termination reveals an abrupt change in sea-surface conditions.

The high abundance of polar *N. pachyderma* in MIS 6 suggests the site was dominated by the cooler waters of the polar front. This is also indicated by the absence of temperate species *G. inflata.*

The Termination is punctuated by H11 but no distinct change in abundances is associated with this large freshwater event. However, this sampling interval may not be sufficiently detailed to define this event.

At the end of the Termination, the peak in *G. inflata* suggests the return of the warm NAC. The migration of warmer waters into this northern latitude is also suggested by the absence of *N. pachyderma* (s) at the onset of MIS 5. *G. bulloides* and *G. inflata* maintain higher abundances in early MIS 5 suggesting sustained warmer sea-surface conditions. During the later phase of MIS 5, *N. pachyderma* (d) reached a peak suggestive of a cooler substage.

The negative $\Delta\delta^{18}O$ values in MIS 5 suggest water column stratification (Mulitza et al., 1997). Stratification at this higher latitude is especially important as it also indicates the presence of a seasonal (spring-summer) thermocline. A warmer sea-surface at this site suggests a strengthening of the NAC by its ability to migrate into higher latitudes. This oceanographic configuration parallels the record expected for an interglacial period.

7) Paleoceanographic Comparison – Subpolar vs. Subtropical

Although cores were taken North (1314) and South (1313) of the "IRD-belt" (Ruddiman, 1977), site 1314 contains a much higher concentration of IRD compared to site 1313. The number of ice-rafted events clearly varies according to geographic location. H11 coincides with an IRD maximum in site 1314 but this is not the case for site 1313 as there are several larger peaks in MIS 6. The IRD peaks of site 1313 in MIS 6 are consistent with other records from a Portuguese margin (Margari et al., 2010) and correspond to depleted $\delta^{18}O$ of planktonic foraminifera suggestive of sea-surface freshening.

In MIS 6, site 1313 has a high diversity foraminiferal species assemblage, with subequal abundances of the species present. In contrast, site 1314 displays a low diversity assemblage dominated by *N. pachyderma* (s), reflecting this species preference for polar waters. The very low abundance of the other species indicates a stressful environment suggesting that sea-surface conditions were too cold for them to thrive. The subtropical location of site 1313 is normally unsuitable for *N. pachyderma* (s), but the glacial conditions create a suitable environment for this species.

H11 generated a differential response between sites. The high sensitivity of *N. pachyderma* (s) to Heinrich Events is attributed to its polar water habitat (Labeyrie et al., 1995). The peaks in *N. pachyderma* and *G. bulloides* in site 1313 suggest the freshwater event cooled the sea-surface at this site allowing these species to reach a temporary peak in abundance. However, H11 did not produce a significant effect at site 1314. This may be due to the already colder conditions associated with higher latitudes. Thus, cooling of the sea-surface will have a more pronounced effect in lower latitudes. At site 1313, higher percentages of *G. bulloides* coincide with cooler sea-surface conditions, whereas at site 1314 it coincides with warmer sea-surface conditions, again demonstrating latitudinal extent of sea-surface variability. *G. inflata* exists in low abundance at site 1313 throughout MIS 6 owing to warmer southern latitudes as opposed to its absence at site 1314 during this time.

At site 1314, the increase of *G. bulloides, G. inflata and N. pachyderma* (d) in MIS 5 suggest a return of warmer surface conditions as these species are associated with the NAC. In MIS 5, site 1314 is characterized by a higher diversity of species with lower abundances. At site 1313, *G. inflata* dominates the assemblage owing to much warmer surface conditions suggestive of a stronger influence of the Gulf Stream.

The nature of the $\delta^{18}O$ curve at the Termination shows a rapid transition at the subpolar site but a more gradual transition at the subtropical site.

8) Conclusions

Paleo-proxy records allowed us to reconstruct the evolution of upper water mass conditions in the North Atlantic across the penultimate deglaciation at a subpolar (1314) and subtropical (1313) location. Two IODP sediment cores were analyzed from MIS 6 to 5. Planktonic foraminfera are well-linked to climatic and environmental conditions in this area and serve as a paleo-proxy. Changes in sea-surface conditions and associated water masses were reflected by changes in foraminiferal relative abundances while $\delta^{18}O$ was used to indicate relative warmer and cooler sea-surface conditions. Iceberg input was monitored by the presence of ice-rafted debris. The variability of the NAC and Polar Front were assessed by inferring the migration of subtropical and subpolar waters. We identified Heinrich Event 11 in both sites which was associated with a massive freshwater release and ensuing perturbation of sea-surface conditions. The warmest sea-surface conditions appear in phase with interglacial MIS 5 and the coolest conditions appear in phase with glacial MIS 6. The supolar site appears to experience a higher magnitude of change in the various proxies used for this study. This suggests that higher latitudes may be more sensitive to climate transitions.

9) Appendix

Table 1

U1313		Composite		sed. wt	Split		# total forams	foram/g	# total IRD	IRD/g	# total Nps	% Nps	# total Npd	% Npd	# total Gb	% Gb	Inflta	% Infla
2H-2WC																		
98-100		565		9.993	2x6	64	34048	3407	64	6	384	1.13	2112	6.20	2816	8.27	896	2.631579
100-102		567		7.29	2x6	64	30720	4214	64	9	512	1.67	960	3.13	3264	10.63	3648	11.875
104-106		571		8.513	2X7	128	65664	7713	384	45	896	1.36	2944	4.48	6912	10.53	1280	1.949318
110-112		577		6.937	2x6	64	26112	3764	64	9	704	2.70	1600	6.13	4992	19.12	2624	10.04902
112-114		579		6.511	2x6	64	24512	3765	64	10	64	0.26	1024	4.18	2368	9.66	896	3.655352
114-116		581		7.725	2x6	64	33088	4283	64	8	192	0.58	2880	8.70	3136	9.48	3968	11.99226
120-122		587		8.672	2x6	64	34688	4000	128	15	64	0.18	1856	5.35	3904	11.25	5184	14.94465
122-124		589		9.687	2x6	64	24512	2530	64	7	64	0.26	1216	4.96	1856	7.57	4160	16.97128
126-128		593		7.482	2x6	64	36160	4833	64	9	64	0.18	1088	3.01	3840	10.62	6912	19.11504
128-130		595		8.217	2x6	64	35776	4354	64	8	192	0.54	1728	4.83	1408	3.94	2304	6.440072
130-132		597		9.373	2x7	128	46080	4916	128	14	128	0.28	3456	7.50	4352	9.44	10624	23.05556
134-136		601		8.35	2x7	128	44672	5350	128	15	256	0.57	1664	3.72	1664	3.72	10368	23.20917
138-140		605		7.792	2x7	128	70144	9002	128	16	128	0.18	3328	4.74	1920	2.74	5248	7.481752
2H-3WC																		
0_2	2	615	6.150	8.102	2x7	128	56704	6999	128	16	384	0.68	2816	4.97	3584	6.32	8448	14.89842
2_4		619		8.527														
4_6		621		7.211	2x7	128	51968	7207	128	18	256	0.49	1152	2.22	2944	5.67	3200	6.157635
6_8	8	623		9.32	2x7	128	64768	6949	128	14	640	0.99	3072	4.74	3840	5.93	9600	14.82213
8_10	10	625		7.99	2x7	128	59264	7417	128	16	640	1.08	2304	3.89	4864	8.21	9344	15.76674
10_12	12	627		6.676	2x7	128	48640	7286	128	19	256	0.53	2304	4.74	5632	11.58	5888	12.10526
12_14	14	629		7.843	2x7	128	40320	5141	128	16	768	1.90	1920	4.76	3328	8.25	5760	14.28571
14_16	16	631		8.532	2x7	128	48768	5716	128	15	896	1.84	1152	2.36	3840	7.87	7424	15.2231
16-18		633		7.627	2x7	128	51072	6696	128	17	1152	2.26	1920	3.76	5120	10.03	8448	16.54135
18-20		635		7.947	2x7	128	45312	5702	256	32	1024	2.26	3584	7.91	4608	10.17	8064	17.79661
20-22	22	637		9.678	2x7	128	56064	5793	128	13	1024	1.83	3840	6.85	6400	11.42	7552	13.47032
22_24		639		8.171	2x6	64	35136	4300	128	16	1728	4.92	2624	7.47	4864	13.84	3072	8.743169
24-26		641		8.396	2x6	64	26048	3102	128	15	960	3.69	2752	10.57	4096	15.72	2176	8.353808
26-28		643		7.45	2x7	128	38528	5172	384	52	3328	8.64	4608	11.96	8064	20.93	2176	5.647841
28-30		645		8.079	2x7	128	47104	5830	128	16	3072	6.52	3328	7.07	13568	28.80	1792	3.804348
30_32		647		6.034	2x7	128	58752	9737	128	21	4224	7.19	3968	6.75	14592	24.84	1920	3.267974
32-34		649		7.716	2x7	128	44032	5707	384	50	2048	4.65	2816	6.40	11520	26.16	1920	4.360465
34-36		651		7.841	2x8	256	92672	11819	512	65	3840	4.14	7168	7.73	26112	28.18	4096	4.41989
36-38		653		7.156	2x7	128	50304	7030	384	54	1664	3.31	2048	4.07	17408	34.61	2304	4.580153
38_40		655		6.478	2x6	64	27136	4189	320	49	1408	5.19	1280	4.72	7680	28.30	896	3.301887
40-42		657		10.246	2x6	64	29056	2836	64	6	640	2.20	1856	6.39	9152	31.50	1280	4.405286
42-44		659		6.237	2x7	128	45312	7265	256	41	1024	2.26	2304	5.08	11520	25.42	3712	8.19209
44-46		661		7.19	2x5	32	15232	2118	160	22	480	3.15	2880	18.91	2624	17.23	1376	9.033613
46_48		663		9.829	2x5	32	10464	1065	32	3	288	2.75	1760	16.82	1472	14.07	896	8.562691
48-50		665		5.944	2x4	16	9616	1618	16	3	112	1.16	1808	18.80	1200	12.48	256	2.66223
54_56		671		6.838	2x5	32	14720	2153	32	5	160	1.09	2944	20.00	1568	10.65	1888	12.82609
60-62		677		9.372	2x5	32	18016	1922	0	0	64	0.36	1920	10.66	1600	8.88	896	4.973357
62_64		679		7.041	2x6	64	20608	2927	64	9	320	1.55	1792	8.70	2688	13.04	2688	13.04348
70_72		687		6.786	2x5	32	11488	1693	224	33	192	1.67	1760	15.32	1440	12.53	1632	14.20613
78_80		695		8.345	2x5	32	15584	1867	608	73	608	3.90	2624	16.84	2400	15.40	1792	11.49897
80-82		697		7.527	2x4	16	7408	984	32	4	112	1.51	1392	18.79	672	9.07	256	3.455724
86_88		703		6.72	2x5	32	11328	1686	128	19	128	1.13	2080	18.36	1280	11.30	1824	16.10169
90-92		707		5.265	2x3	8	2656	504	16	3	8	0.30	648	24.40	176	6.63	128	4.819277
94_96		711		6.57	2x5	32	11136	1695	32	5	288	2.59	2848	25.57	768	6.90	1216	10.91954
100-102		717		7.395	2x6	64	19648	2657	0	0	256	1.30	3968	20.20	3392	17.26	512	2.605863
102_104		719		7.552	2x6	64	30592	4051	192	25	384	1.26	6144	20.08	5760	18.83	1408	4.60251
110_112		727		6.594	2x7	128	50176	7609	512	78	1408	2.81	6784	13.52	9344	18.62	2816	5.612245
118_120		735		6.508	2x7	128	72320	11112	384	59	2688	3.72	4864	6.73	13056	18.05	2048	2.831858
120-122		737		6.583	2x7	128	54016	8205	384	58	1280	2.37	5120	9.48	9600	17.77	128	0.236967
122-124		739		6.95	2x7	128	49280	7093	1024	147	1280	2.60	3200	6.49	8960	18.18	1536	3.116883
126_128		743		7.201	2x8	256	81920	11376	1024	142	3072	3.75	8704	10.63	14848	18.13	2560	3.125
130-132		747		7.203	2x7	128	44032	6113	512	71	1792	4.07	2816	6.40	6144	13.95	128	0.290698
134_136		751		6.704	2x7	128	66176	9871	768	115	2176	3.29	4480	6.77	11392	17.21	384	0.580271
140_142		757		5.596	2x6	64	36032	6439	384	69	1024	2.84	3584	9.95	3392	9.41	1216	3.374778
148_150		764		7.50	2x7	128	54144	7219	512	68	1152	2.13	7168	13.24	2432	4.49	896	1.654846
2H-4WC																		
0-2		765		4.86	2x7	128	46080		384		512	1.11	4736	10.28	384	0.83	128	0.277778
10-12.		777		7.03	2x7	128	75136		384		384	0.51	4736	6.30	4992	6.64	896	1.192504
16-18		783		6.83	2x8	256	135168		1024		512	0.38	7424	5.49	16384	12.12	2816	2.083333
24-26		791		6.98	2x6	64	42176		192		256	0.61	3520	8.35	3904	9.26	320	0.758725
32-34		799		9.37	2x7	128	59904		384		512	0.85	11648	19.44	4096	6.84	1664	2.777778
40-42		807		9.48	2x7	128	84352		128		768	0.91	9344	11.08	7936	9.41	2688	3.186646
48-50		815		9.85	2x7	128	82176		768		384	0.47	3072	3.74	6016	7.32	1536	1.869159
56-58		823		9.74	2x8	256	101376		768		1536	1.52	6400	6.31	10752	10.61	1024	1.010101
64-66		831		8.54	2x7	128	65152		768		1280	1.96	4096	6.29	5376	8.25	768	1.178782
72-74		839		7.39	2x7	128	68992		1792		1152	1.67	5888	8.53	5376	7.79	1152	1.669759
80-82		847		14.91	2x7	128	50944		1152		2048	4.02	4992	9.80	5120	10.05	512	1.005025
88-90		855		7.25	2x6	64	30848		192		1152	3.73	5568	18.05	3008	9.75	640	2.074689
96-98		863		6.22	2x6	64	28672		64		192	0.67	3648	12.72	1408	4.91	1088	3.794643
104-106		871		6.01	2x6	64	35648		128		64	0.18	9216	25.85	1280	3.59	768	2.154399
112-114		879		7.23	2x5	32	21568		32		96	0.45	3104	14.39	992	4.60	960	4.451039
120-122		887		6.69	2x5	32	12640		32		0	0.00	2016	15.95	448	3.54	576	4.556962
128-130		895		6.26	2x5	32	16224		32		64	0.39	2560	15.78	864	5.33	288	1.775148
136-138		903		8.90	2x6	64	38976		64		128	0.33	4160	10.67	1856	4.76	2432	6.239737
144-146		911		9.09	2x7	128	82816		128		512	0.62	2816	3.40	5248	6.34	2560	3.09119
148-150		915		14.04	S	256	123648		256		512	0.41	6912	5.59	12544	10.14	3072	2.484472

Table 2

U1314		Composite		sed. wt	Split		# total forams	foram/g	# total IRD	IRD/g	# total Nps	% Nps	# total Npd	% Npd	# total Gb	% Gb	Inflta	% Infla
2H-1W																		
122-124		1000		6.485565	2x8	256	131072	20210	768	118	12032	9.18	2048	1.56	3328	2.54	768	0.585938
132-134		1010		6.887917	2x8	256	133632	19401	256	37	2816	2.11	3584	2.68	5376	4.02	0	0
140-142		1018		5.491491	2x7	128	58368	10629	128	23	2304	3.95	2304	3.95	1920	3.29	1024	1.754386
148-150		1026		5.97	2x6	64	38464	6443	128	21	320	0.83	2752	7.15	1344	3.49	1024	2.66223
2H-2W																		
0-2		1028		3.102559	2x4	16	9840	3172	32	10	48	0.49	512	5.20	64	0.65	624	6.341463
8.-10		1036		2.433778	2x6	64	22592	9283	64	26	256	1.13	4416	19.55	512	2.27	1280	5.665722
20-22		1048		3.586022	2x6	64	30720	8567	64	18	0	0.00	11008	35.83	384	1.25	192	0.625
28-30		1056		2.50572	2x6	64	34176	13639	64	26	256	0.75	12352	36.14	1280	3.75	640	1.872659
40-42		1068		3.133877	2x6	64	29824	9517	64	20	128	0.43	8704	29.18	960	3.22	1024	3.433476
48-50		1076		2.854163	2x6	64	33600	11772	64	22	128	0.38	8640	25.71	1344	4.00	960	2.857143
58-60		1086		3.542874	2x7	128	47232	13332	128	36	0	0.00	9344	19.78	3328	7.05	2176	4.607046
66-68		1094		4.592197	2x7	128	69632	15163	128	28	0	0.00	16000	22.98	5760	8.27	896	1.286765
76-78		1104		4.727199	2x8	256	89088	18846	256	54	0	0.00	13824	15.52	5376	6.03	3328	3.735632
86-88		1114		6.09163	2x8	256	111872	18365	256	42	512	0.46	19456	17.39	6400	5.72	4864	4.347826
96-98		1124		4.394604	2x7	128	44544	10136	128	29	128	0.29	11136	25.00	2048	4.60	1664	3.735632
104-106		1132		4.460249	2x7	128	69248	15526	128	29	128	0.18	17280	24.95	4992	7.21	2304	3.327172
116-118		1144		6.198724	2x8	256	91392	14744	256	41	0	0.00	18688	20.45	4608	5.04	3328	3.641457
126-128		1154		4.95811	2x7	128	82944	16729	128	26	0	0.00	19072	22.99	2816	3.40	1024	1.234568
138-140		1166		4.676019	2x7	128	91008	19463	128	27	0	0.00	25984	28.55	7040	7.74	512	0.562588
144-146		1172	11.72	4.664783	2x7	128	63744	13665	128	27	128	0.20	5248	8.23	5760	9.04	1792	2.811245
148-150		1176	11.76	5.227725	2x7	128	67328	12879	0	0	0	0.00	8064	11.98	7168	10.65	3072	4.562738
2H-3W																		
0_2	2	1178	11.78	4.78	2x7	128	67584	14140	128	27	0	0.00	8320	12.31	7808	11.55	2560	3.787879
8_10		1186	11.86	4.10	2x8	256	77056		768		0	0.00	8448	10.96	10240	13.29	1792	2.325581
16_18		1194	11.94	3.43	2x8	256	84224		256		512	0.61	10496	12.46	11008	13.07	8448	10.0304
18-20		1196	11.96	3.84	2x7	128	73728		128		512	0.69	17408	23.61	8832	11.98	1280	1.736111
24_26		1202	12.02	3.94	2x8	256	144384		256		256	0.18	14592	10.11	24320	16.84	10752	7.446809
28-30		1206	12.06	5.04	2x8	256	109056		256		0	0.00	37120	34.04	10240	9.39	1024	0.938967
32_34		1210	12.10	4.28	2x8	256	80384		256		768	0.96	15872	19.75	7168	8.92	5888	7.324841
34_36		1212	12.12	5.27	2x8	256	119296		256		0	0.00	17920	15.02	13312	11.16	11008	9.227468
38-40		1216	12.16	4.54	2x8	256	98048		256		0	0.00	39680	40.47	6400	6.53	1792	1.827676
40_42		1218	12.18	5.14	2x8	256	90368		256		512	0.57	17664	19.55	4864	5.38	4352	4.815864
48_50		1226	12.26	7.80	2x7	128	48640		896		640	1.32	9344	19.21	4608	9.47	3328	6.842105
50-52		1228	12.28	6.727014	2x8	256	95488		2816		256	0.27	33280	34.85	2560	2.68	1792	1.876676
52-54		1230	12.30	7.41541	2x8	256	103936		5376		4352	4.19	18176	17.49	7168	6.90	9984	9.605911
54-56		1232	12.32	10.26211														
56_58		1234	12.34	10.59	2x8	256	122112		12800		6400	5.24	20224	16.56	6912	5.66	16384	13.41719
58-60		1236	12.36	17.45														
60-62		1238	12.38	25.24	2x8	256	93184		48640		11264	12.09	13568	14.56	3072	3.30	7680	8.241758
62-64		1240	12.40	2.81	2x8	256	90368		26624		12288	13.60	11520	12.75	3584	3.97	11520	12.74788
64_66		1242	12.42	14.96	2x7	128	47104		20352		9472	20.11	4864	10.33	2688	5.71	3200	6.793478
66-68		1244	12.44	14.59	2x7	128	56192		28544		8576	15.26	6144	10.93	7936	14.12	5376	9.567198
68-70		1246	12.46	19.79	2x7	128	40192		72320		19328	48.09	3328	8.28	1280	3.18	1664	4.140127
70-72		1248	12.48	18.47	2x5	32	8512		35296		2880	33.83	640	7.52	128	1.50	512	6.015038
80_82		1258	12.58	13.36	2x9	512	147968		16896		73216	49.48	4096	2.77	8192	5.54	1536	1.038062
90-92		1268	12.68	15.92	2x8	256	124672		8960		66304	53.18	2304	1.85	5376	4.31	0	0
100_102		1278	12.78	18.16	2x8	256	108288		7936		57344	52.96	1024	0.95	2048	1.89	0	0
110-112		1288	12.88	18.07	2x9	512	207872		27136		94208	45.32	0	0.00	10752	5.17	0	0
120_122	16	1298	12.98	14.73	2x9	512	288768		11264		72192	25.00	10240	3.55	36352	12.59	3072	1.06383
130-132		1308	13.08	21.35	2x9	512	204288		21504		101376	49.62	1024	0.50	9216	4.51	512	0.250627
140_142	8	1318	13.18	22.01	2x9	512	200192	9095	24064	1093	89600	44.76	3584	1.79	0	0.00	0	0
2H-4W																		
0_2		1328	13.28	13.84478	2x8	256	121088		4352		34048	28.12	4352	3.59	7424	6.13	256	0.211416

References

1. Bé, A. W. H, and Tolderlund, D. S. (1971). Distribution and ecology of living planktonic foraminifera in surface waters of the Atlantic and Indian Oceans, In: The Micropaleontology of Oceans, Cambridge University Press, NY, pp. 105-149.

2. Bond, G., and Lotti, R. (1995). Iceberg discharges into the North Atlantic on millennial time scales during the last deglaciation. *Science* **267**, 1005-1010.

3. Broecker, W.S., Bond, G., Klas, M., Bonani, G., and Wolfi, W. (1990). A salt oscillator in the North Atlantic? *Paleoceanography* **5**, 469-477.

4. Cléroux, C., Cortijo, E., Duplessy, J-C., and Zahn, R. (2007) Deep-dwelling foraminifera as thermocline temperature recorders. *Geochemistry, Geophysics, Geosystems.* **8**, doi: 10.1029/2006GC001474.

5. Cléroux, C., E. Cortijo, P. Anand, L. Labeyrie, F. Bassinot, N. Caillon, and J.-C. Duplessy (2008). Mg/Ca and Sr/Ca ratios in planktonic foraminifera: Proxies for upper water column temperature reconstruction. *Paleoceanography* **23**, doi:10.1029/2007PA001505.

6. Dansgaard, W., Oeschger, H., Langway, C.C. (1983) Ice core indications of Abrupt Climate Changes. *Palaeoclimate Research and Models; report and proceedings, workshop*. 72-73.

7. Emiliani, C. (1966). Isotopic Paleotemperatures. *Science* **154**, 851-857.

8. Heinrich, H. (1988). Origin and consequences of cyclic ice rafting in the northeast Atlantic Ocean during the past 130,000 years. *Quaternary. Res.* **29**, 142-152.

9. Johannessen, T., Jansen, E., Flatoy, A., and Ravelo, A. (1993) The Relationship Between Surface Water Masses, Oceanographic Fronts and Paleoclimatic Proxies in Surface Sediments of the Greenland, Iceland, Norwegian seas. *Carbon cycling in the glacial ocean: Constraints on the ocean's role in global change.* NATO ASI Series (Vol. 17, pp.61-85). Berlin: Springer.

10. Kennett, J.P., and Srinivasan, M.S. (1983). Neogene Planktonic Foraminifera: A phylogenetic Atlas. Hutchinson Ross Publishing Co.

11. Kreveld, S.A. van. (1996). Northeast Atlantic Late Quaternary planktic foraminifera as a primary productivity and water mass indicators. *Scripta Geol.* **113**, 23-91.

12. Kukla, G.J., Michael, L., Bender, J.-L., et al. (2002a). Last interglacial climates. *Quat. Res.* **58**, 2-13.

13. Labeyrie, L., Leclaire, H., Waelbroeck, C., Cortijo, E., Duplessy, J.-C., Vidal, L., Elliot, M., and Le Coat, B. (1999). Temporal Variability of the Surface and Deep Waters of the North West Atlantic Ocean at Orbital and Millenial Scales. *Mechanisms of Global Climate Change at Millennial Time Scales: Geophysical Monograph.* **112**, 77-112**.**

14. Lisiecki, L. E. and Raymo, M. E., (2005). A Pliocene-Pleistocene stack of 57 globally distributed benthic $\delta^{18}O$ records. *Paleoceanography* **20**, doi:10.1029/2004PA001071.

15. Margari,V., L. C. Skinner, P. C. Tzedakis, A. Ganopolski, M. Vautravers, and N. J. Shackleton (2010). The nature of millennial-scale climate variability during the last two glacial periods. *Science* **3**, 127-131.

16. Milankovitch, M. (1941). Canon on Insolation and the Ice-Age Problem. *Royal Serbian Academy, Special Publication,* Vol. **132**. Translation (1969), Israel Academy Program for Scientific Translation, Jerusalem.

17. Mulitza, S., Dürkoop, A., Hale, W., Wefer, and G., Niebler, H.S. (1997) Planktonic foraminifera as recorders of past surface-water stratification. *Geology* **25**, 335-338.

18. Ottens, J. J. (1991). Planktic foraminifera as North Atlantic water mass indicators, *Oceanologica Acta* **14**, 123-140.

19. Rashid, H., and Boyle, E. (2007). Mixed Layer Deepening During Heinrich Events: A Multi-Planktonic Foraminiferal $\delta^{18}O$ approach. *Science* **318**, 439-441.

20. Rashid, H., and Boyle, E. (2008). Response to the comment on "Mixed-layer deepening during Heinrich Events: a multi-planktonic foraminiferal $\delta^{18}O$ approach". *Science* **320**, 1161-1162.

21. Ruddiman, W. F. (1977). Late Quaternary deposition of ice-rafted sand in the subpolar North Atlantic (40-65oN), Geol. Soc. Am. Bull. **88**, 1813-1827.

22. Ruddiman, W. (2008) Earth's Climate Past and Future. W.H. Freeman and Company. 2nd Ed.

23. Serreze, M., and Barry, G. (2005). *The Arctic Climate System* Cambridge University Press. Arctic Paleoclimates, pp.262-290.

24. Shackelton, N.J., Fernanda Sanchez-Goni, M., Pailler, D., and Lancelot, Y. (2003). Marine Isotope Substage 5e and the Eemian Interglacial. *Global Planet. Change* **36**, 151-155.

25. Thornalley, D., Elderfield, and H., and McCave, N. (2009) Holocene oscillations in temperature and salinity of the surface subpolar North Atlantic. *Nature* **457**, doi:10.1038/nature07717.